V.N.1 Transport Phenomena and Interfacial Kinetics in Planar Microfluidic Membraneless Fuel Cells

Héctor D. Abruña[1], Abraham Stroock[2],
[1]Department of Chemistry & Chemical Biology
[2]Department of Chemical Engineering
Cornell University
Ithaca, NY 14853

DOE Program Officer: Richard D. Kelley
Phone: (301) 903-6051
E-mail: Richard.Kelley@science.doe.gov

Objectives

Develop a fundamental understanding of transport behavior in planar microfluidic membraneless fuel cells. Design and implement staggered herringbone micromixers to enhance mass transport while maintaining laminar flow. Identify novel fuel/oxidant couples to optimize power output.

Technical Barriers

Enhance the fuel utilization efficiency of planar microfluidic membraneless fuel cells through simulation of transport behavior under various electrode geometries, and the design and implementation of the novel micromixer designs. Identify appropriate fuel/oxidant combinations with fast charge transfer kinetics, which can also provide high fuel cell voltages and current densities.

Abstract

We have carried out investigations geared toward the fundamental understanding of the transport behavior in planar microfluidic membraneless fuel cells with the intent of locally enhancing mass transport, while maintaining laminar flow between fuel and oxidant streams. In order to accomplish this, we have employed staggered herringbone micromixers which were generated using microfabrication techniques. We have also carried out preliminary electrochemical testing of these micromixers. In order to obtain high voltages and high power from these planar microfluidic membraneless fuel cells, we have investigated and characterized a number of fuel/oxidant combinations with fast charge transfer kinetics. Finally, due to its attractive nature as a fuel, we have carried out a thorough study of the activation energy of methanol oxidation at a platinum electrode in acid and alkaline media.

Progress Report

We have fabricated electrodes that present the staggered herringbone motif. The electrode substrate is borosilicate glass in which grooves are etched with buffered hydrofluoric acid through a solid mask. Figure 1A presents a scanning electron micrograph of the herringbone structures in the glass substrate. The width of the structure is 1 mm and the length is 5 cm. The features were etched into the glass about 50 microns in depth and the features were rounded due to the isotropic nature of the chemical etch. The surfaces were subsequently cleaned and metallized by evaporation and electroplating to form highly conductive and catalytically active electrodes. Figure 1B presents an optical micrograph of a gold coated structured electrode.

These electrodes were mounted in a flow cell with a PDMS microchannel and tested using chronoamperometry, with $Na_4[Fe(CN)_6]$ as the redox active component, while varying the flow rate; the electrochemical system is illustrated schematically in Figure 2A. This geometry allowed us to quantify the impact of the three-dimensional flows generated by the structured electrodes on the diffusion-limited current, and to compare our published predictions (1). We operated the cell in three configurations, as shown schematically as insets in Figure 2B: 1) with flat working and counter electrodes; 2) with a grooved counter and a flat working; in this case the stirring flows are generated on the boundary opposite the limiting electrode; and 3) with a grooved working electrode; in this case the stirring flows originate from the limiting electrode. These results present the total current versus non-dimensional flow speed, *Pe* in a cell of height, *H*,

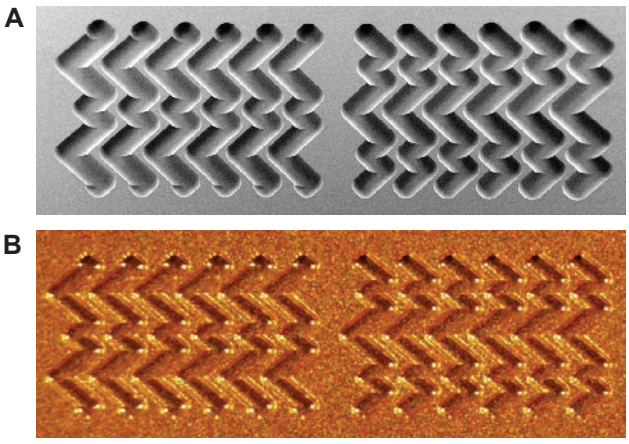

FIGURE 1. Chaotic Electrodes

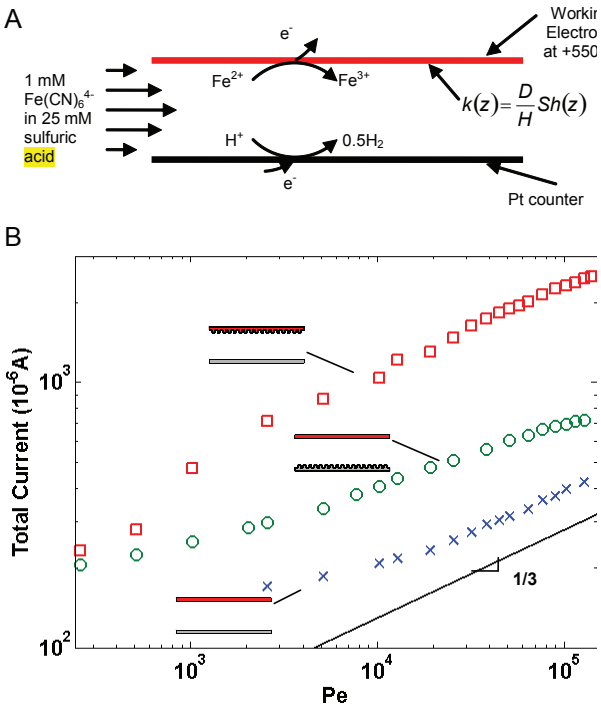

FIGURE 2. Characterization of transport limited current controlled by chaotic electrodes in a potential cell. **(A)** Schematic diagram of electrochemical cell operated in diffusion-limited regime with oxidation of ferrocyanide at the working electode. The reference electrode was placed in the outlet reservoir. **(B)** Total current versus Péclet, $Pe = UH/D$, where U is the average flow speed, H is the height of the channel, and D is the diffusivity of ferrocyanide. Data from three configurations is shown: flat working with flat counter (×), grooved counter and flat working (○), and flat counter and grooved working (□).

length, L, and depth, W. The total current is of the following form:

$$I = FC_0WL\frac{D}{H}Sh_L ,$$

where F is Faraday's constant, C_0 and D are the incoming concentration and diffusivity of ferrocyanide, and Sh_L is the global Sherwood number, a measure of the efficiency of mass transfer. Our predictions for Sh_L based on results in ref. 1 are presented in the following table.

flat counter – flat working	$\frac{3}{2}\left(\frac{H}{L}\right)^{1/3} Pe^{1/3} = 0.19Pe^{1/3}$
groved counter – flat working	$\left(\frac{H}{W}\right)^{1/3}\left(\frac{H\dot{\gamma}_{trans}}{U_{trans}}\right)^{1/3}\left(\frac{U_{trans}}{U}\right)^{1/3} Pe^{1/3}$ $= 0.46Pe^{1/3}$
flat counter – groved working	$\left(\frac{grooved\ area}{flat\ area}\right)\left(\frac{H}{W}\right)^{1/3}\left(\frac{H\dot{\gamma}_{trans}}{U_{trans}}\right)^{1/3}\left(\frac{U_{trans}}{U}\right)^{1/3} Pe^{1/3}$ $= 0.80Pe^{1/3}$

Most importantly, the results in Figure 2B indicate that a grooved electrode can generate a five fold or greater increase in current relative to a flat electrode at the same flow rate. The results are also comparable to the predicted scaling and prefactors for the two cases with flat working electrode; we are currently working clarifying the exact behavior when the grooved electrode is limiting.

We have also investigated the use of various fuel/oxidant combinations in order to enhance the power output of the planar microfluidic membraneless fuel cells. Our initial studies (1) had focused on the use of formic acid as a fuel with oxygen as oxidant. However, the power outputs were relatively modest. We then studied the hydrogen/oxygen system since it represented one of the most widely studied. Of particular note in these early studies was the use of dual electrolyte system (2) in which the fuel stream (anode) was alkaline while the oxidant stream (cathode) was acidic. This asymmetry allowed for open circuit single cell voltages in excess of 1.4V.

We have also studied additional fuel/oxidant combinations the first of which was the methanol (0.5M)/O_2 fuel cell system. We carried out studies in acidic, alkaline and dual electrolyte configurations and the results are presented in Figure 3. As Figure 3 shows, the performance in alkaline media was superior to that in acidic electrolyte, as anticipated based on the improved kinetics and thermodynamics. Moreover, the dual electrolyte system exhibited dramatic improvements over the single electrolyte systems both in terms of current density and open circuit potentials. These improvements translated into significantly larger power outputs in the dual electrolyte configuration.

The other fuel/oxidant combination that we have studied in some detail is the sodium borohydride

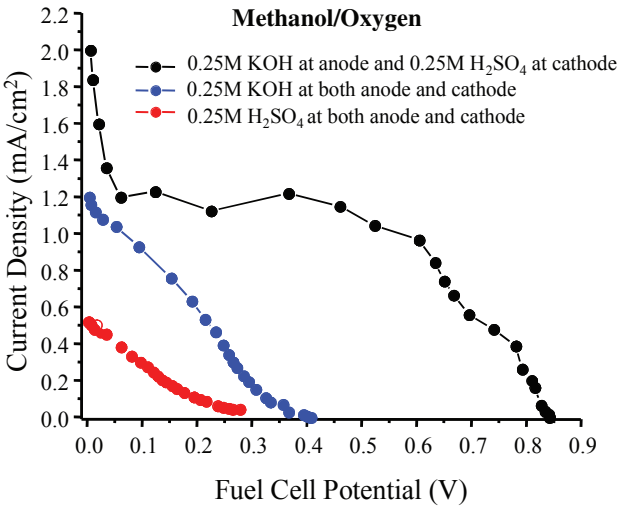

FIGURE 3.

(BH_4^-), hydrogen peroxide (H_2O_2) system. This system is particularly attractive because the fuel (BH_4^-) can, in principle, provide eight electrons per mole and in addition, both fuel and oxidant are highly soluble in aqueous media. Moreover the system also lends itself to the dual electrolyte configuration. Figure 4 presents a family of current density/voltage profiles for the (BH_4^-)/(H_2O_2) system at different concentrations and in the dual electrolyte configuration. For comparison, the (BH_4^-)/(O_2) system is also presented. Upon inspection, it is immediately evident that the (BH_4^-)/(H_2O_2) system exhibits superior performance. In fact, the output exceeds 12mW/cm^2.

Finally, and in an effort to better understand, from a mechanistic standpoint, the oxidation of methanol at a platinum electrode surface, we have carried out a detailed study and analysis of the activation energies involved under a variety of experimental conditions including pH, applied potential and surface coverage of oxygenated species (3). From these studies (Figure 5) we have been able to develop a clearer picture of the coupling of these various dependencies and how these may provide valuable insights for the development of better electrocatalysts.

Future Directions

Over the next year out efforts will be focused on:

- Further development, implementation and testing, under realistic fuel cell operating conditions of the staggered herringbone micromixers.
- Computational and simulation studies of the transport phenomena involved in the use of the staggered herringbone micromixers.
- Further studies and implementation of the borohydride/hydrogen peroxide system.
- Output optimization of single and stacked planar membraneless fuel cells.

References

1. Kirtland, J. D.; McGraw, G. J.; Stroock, A. D. Mass Transfer to Reactive Boundaries from Steady Three-Dimensional Flows in Microchannels. Physics of Fluids (2006), *18*, 073602.

2. Cohen, J. L.; Westly, D. A.; Pechenick, A. and Abruña, H. D. "Fabrication and Preliminary Testing of a Planar Membraneless Microchannel Fuel Cell" J. Power Sources, Sources (2005), 139(1-2), 96-105.

3. Cohen, J. L.; Volpe, D. J.; Westly, D. A.; Pechenick, A. and Abruña, H. D. "A Dual Electrolyte H_2/O_2 Planar Membraneless Microchannel Fuel Cell System with Open Circuit Potentials in Excess of 1.4 V" Langmuir (2005), 21(8), 3544-3550.

4. Cohen, Jamie L.; Volpe, David J.; Abruna, Hector D.. Electrochemical determination of activation energies for methanol oxidation on polycrystalline platinum in acidic and alkaline electrolytes. Physical Chemistry Chemical Physics (**2006**), 9(1), 49-77.

Publications (Including Patents) Acknowledging the Grant or Contract

1. Cohen, Jamie L.; Volpe, David J.; Abruña, Héctor D.. Electrochemical determination of activation energies for methanol oxidation on polycrystalline platinum in acidic and alkaline electrolytes. Physical Chemistry Chemical Physics (2006), 9(1), 49-77.

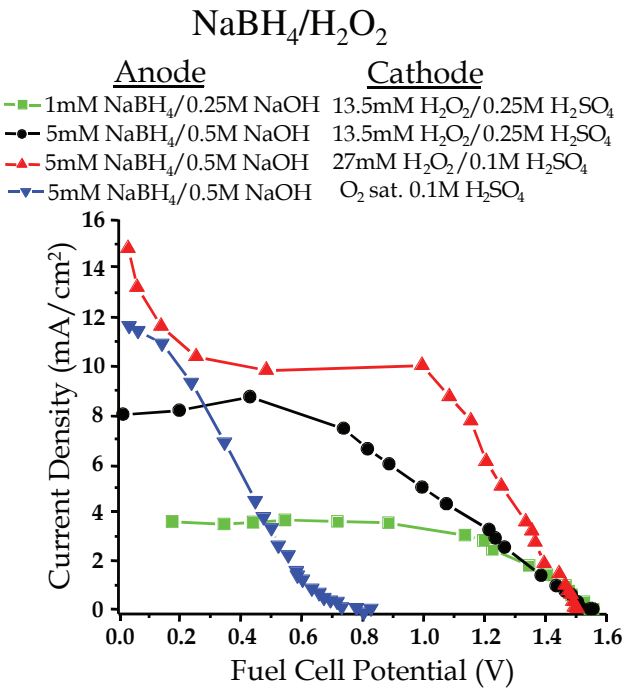

FIGURE 4.

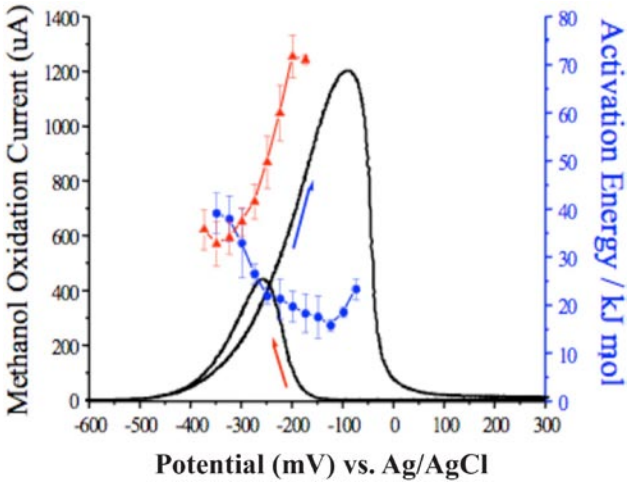

FIGURE 5.

2. Kirtland, J. D.; McGraw, G. J.; Stroock, A. D. Mass Transfer to Reactive Boundaries from Steady Three-Dimensional Flows in Microchannels. Physics of Fluids (2006), *18*, 073602.